Physica A 421 (2015) 261–268

Contents lists available at ScienceDirect

Physica A

journal homepage: www.elsevier.com/locate/physa

Percolation of dimers irreversibly adsorbed on heterogeneous surfaces

M.C. Gimenez [a,*], A.J. Ramirez-Pastor [b]

[a] Facultad de Matemática, Astronomía y Física, U.N.C., Córdoba, IFEG - CONICET, Argentina

[b] Departamento de Física, Instituto de Física Aplicada, Universidad Nacional de San Luis - CONICET, Ejército de Los Andes 950, D5700HHW, San Luis, Argentina

HIGHLIGHTS

- The percolation problem of deposited dimers on square lattices is studied.
- The surfaces are generated by square patches, which can be ordered or random.
- Dimers are irreversibly adsorbed on the lattice.
- At high coverage, the final state generated is a disordered state.
- The curves separating the percolating and non-percolating regions were calculated.

ARTICLE INFO

Article history:
Received 26 August 2014
Received in revised form 10 November 2014
Available online 20 November 2014

Keywords:
Percolation
Dimers
Adsorption
Heterogeneous surfaces

ABSTRACT

The percolation problem of irreversibly deposited dimers on square lattices with two kinds of sites is studied. Simple adsorptive surfaces are generated by square patches of $l \times l$ sites, which can be either arranged in a deterministic chessboard structure or in a random way. Thus, the system can be characterized by the distribution (ordered or random) of the patches, the patch size l and the probability of occupying each patch θ_i ($i = 1, 2$). Dimers (particles that occupy two neighboring sites simultaneously) are irreversibly adsorbed on the lattice. By means of random adsorption simulations and finite-size scaling analysis, a complete (θ_1–θ_2–l) phase diagram separating a percolating and a non-percolating region is determined.

1. Introduction

Percolation theory has been investigated in the last few decades and it is still a topic of great interest [1–27]. It studies the emergence of long-range connectivity in many systems such as network theory [2,13–17], the flow and transport in porous media [2,4,19], transport in disordered media [18,19], spread of disease in populations [20], forest fires [21], spread of computer viruses [23], network failures [24,25], formation of gels [22], and even formation of social groups [26,27]. The percolation threshold is defined as the minimum concentration at which an infinite cluster of occupied elements spans the system.

Most of the studies of percolation have taken into account that the state of sites on lattice changes irreversibly from empty to filled (occupied). In these cases, the temperature of the system does not play any relevant role and it is not considered. Another interesting application of percolation theory is related to the description of the spatial distribution of particles adsorbed (in equilibrium) on solid surfaces [28–31]. In this framework, Giménez et al. studied the percolation properties of

* Corresponding author.
E-mail address: cgimenez@famaf.unc.edu.ar (M.C. Gimenez).

http://dx.doi.org/10.1016/j.physa.2014.11.036
0378-4371/

the adsorbed phase of (1) interacting monomers on square, honeycomb and triangular lattices [28,29]; (2) interacting dimers on square lattices [29]; (3) non-interacting monomers on heterogeneous surfaces [30]; and (4) interacting monomers on heterogeneous surfaces [31].

Despite of the number of contributions to the percolation problem, there are many aspects which are not yet completely solved. In fact, most of the studies are devoted to the percolation of objects whose size coincides with the size of the lattice site (single occupancy). However, if some sort of correlation exists, like particles occupying several k contiguous lattice sites (k-mers), the statistical problem becomes exceedingly difficult and a few studies have been devoted to understanding the percolation of elements occupying more than one site (bond) [8,9,32,33].

In Refs. [8,9,32], the percolation behavior for k-mers with a length in the interval $k = 1, \ldots, 15$ has been studied. The authors found that the percolation threshold exhibits an exponentially decreasing behavior as a function of the k-mer size. This feature was observed for straight and tortuous k-mers deposited on 2D square lattices [8,9], and for straight k-mers on 3D cubic lattices [32]. In all the studied cases, the problem was shown to belong to the random percolation universality class. Nevertheless, in a recent work by Tarasevich et al. [33] a nonmonotonic size dependence was observed for the percolation threshold of straight k-mers on 2D square lattices, which decreases for small particles sizes, goes through a minimum at $k \approx 13$, and finally increases for large segments.

In all of the cases mentioned above, the particles are always deposited on a homogeneous surface. This means that all the sites are considered to have the same probability of occupation as they are "seen" by the incoming particles. However, it has been shown that even single crystal surfaces are not perfect and contain structural and energetic heterogeneities which clearly indicate the necessity to develop more refined atomistic models for describing heterogeneous surfaces and for studying the processes taken place on them as well. In this line, the percolation of monomers (single particles that occupy each one single site) on heterogeneous surfaces was investigated by Nieto et al. [34]. The authors presented a simple model in which two types of independent sites are located either in a chessboard structure or in random patches. The composition of this system was characterized by the occupation probabilities of each type of site θ_1 and θ_2. Interesting $(\theta_1 - \theta_2)$ phase diagrams were obtained and discussed.

The aim of the present paper is to investigate the combined effect of multisite occupancy and heterogeneity. For this purpose, dimers (particles that occupy two adjacent lattice sites) are irreversibly deposited on patchwise lattices. These lattices, largely used to model adsorptive heterogeneous surfaces, are composed of two different types of sites, which in turn are grouped into homogeneous patches or finite domains.

From an experimental point of view, numerous studies show that on some kinds of metal surfaces, molecular adsorption is the initial step and is followed by dissociation [35,36]. In all cases, when the diatomic molecule dissociates, it is broken into two monomers, each of which occupies a site. The distributions of such dissociated monomers and the structure of the clusters composed of them are important in the catalytic processes. Because the dimers are randomly placed on the lattice and randomly dissociate, the dissociative adsorption is a spatial random process. Therefore, it can be clearly illustrated by dimer percolation models [37].

On the other hand, simple heterogeneous surfaces as studied here, have also been intensively used in modeling adsorption phenomena [38]. A special class of bivariate surfaces, with a chessboard structure, has been observed to occur in a natural system [39]. Bivariate surfaces may also mimic, to a rough approximation, more general heterogeneous surfaces with energetic topography arising from a solid where a small amount of randomly distributed impurity (strongly adsorptive) atoms are added [40].

This paper is organized as follows: in Section 2 we describe the model and the simulation technique used to obtain the desired quantities for describing the percolation phase transition. Results are presented and discussed in Section 3. Finally, some conclusions are drawn in Section 4.

2. Model and calculation method

The heterogeneity of the system is characterized by two parameters: the patch size l and the probability of occupying each patch θ_i $(i = 1, 2)$. The deposition of the dimers is followed by the calculation of the percolation properties by means of the Hoshen–Kopelman algorithm [41]. For each pair (θ_1, θ_2) the percolation probability is obtained by averaging over 10 000 samples. The procedure is repeated for several system sizes in order to make a finite-size analysis and extrapolate the percolation probability for an infinite system.

Let us consider the substrate is represented by a two-dimensional square lattice of $M = L \times L$ sites with periodic boundary conditions. There are two kinds of sites: sites 1 and sites 2, in equal concentration. These sites form square patches of size l $(l = 1, 2, 3, \ldots)$ which are spatially distributed either in a deterministic alternate way (chessboard topography), or in a nonoverlapping random way (random topography).

In order to easily identify a given topography, we introduce the notation l_C for a chessboard topography of size l and, similarly, l_R for random square patches.

Given θ_1 and θ_2, the occupancy probability of each kind of site, the lattice is filled with dimers until $\theta_1 \times M/2$ sites of kind 1 and $\theta_2 \times M/2$ sites of kind 2 are occupied. The procedure is the following. (1) One lattice site is chosen at random. (2) If the site selected in (1) is empty, then one of his four neighboring sites is selected at random. (3) If both sites are unoccupied, a dimer is deposited on those two sites. (4) Steps (1)–(3) are repeated until the two probabilities θ_1 and θ_2 are satisfied or until

jamming conditions. Due to the blocking of the lattice by the already randomly deposited dimers, the limiting or jamming coverage, $\theta^J_{1(2)} = \theta_{1(2)}(t \to \infty)$ is less than that corresponding to the close packing ($\theta^J_{1(2)} < 1$).

If the coverage of sites type 1 reaches the maximum value (θ_1), the step involving adsorption on type 1 sites is rejected and the procedure is repeated until the coverage of type 2 sites reaches the value θ_2, and vice versa.

An extensive overview of this field can be found in the excellent work by Evans [42] and references therein.

The central idea of the percolation theory is based on finding the minimum coverage degree for which at least a cluster (a group of occupied sites in such a way that each one of them has at least one occupied nearest neighbor site) extends from one side to the opposite one of the system. This particular value of the coverage degree is named *critical concentration* or *percolation threshold* and determines a phase transition in the system. In the present model, given θ_1, we look for the value of θ_2 for which percolation occurs, and that value will be our percolation threshold θ_2^c.

As the scaling theory predicts [10], the larger the system size to study, the more accurate the values of the threshold obtained therefrom. Thus, the finite-size scaling theory give us the basis to achieve the percolation threshold and the critical exponents of a system with a reasonable accuracy. For this purpose, the probability $R = R_L^U(\theta)$ that a lattice composed of $L \times L$ sites percolates at concentration θ can be defined [2,43,44]. $R_L^U(\theta)$ is the probability of finding either a rightward **or** a downward percolating cluster.

In the simulations, each run consists of the following steps: (a) the construction of the lattice for the desired fraction (θ_1, θ_2), according to the scheme mentioned before, and (b) the cluster analysis by using the Hoshen and Kopelman algorithm [41]. n runs of such two steps are carried out for obtaining the number m^U of them for which a percolating cluster is found. Then, $R_L^U(\theta_2) = m^U/n$ is defined and the procedure is repeated for a fixed value of θ_1 and different values of θ_2. A set of $n = 10\,000$ independent samples is numerically prepared for each pair (θ_1, θ_2), l and L.

The present percolation study involves dimers irreversibly adsorbed on heterogeneous surfaces characterized by the linear dimension L and the patch size l. The value of L has to be properly chosen such that the adlayer structure is not perturbed, and considering the number and ordering of the energetic patches and their size l. Thus, L must be even and multiple of $2l$. In our calculations we have used $L = 32, 48, 64, 80, 96, 112, 128$ for $l = 2$, $L = 36, 48, 60, 72, 96, 120, 144$ for $l = 3$, $L = 40, 48, 64, 80, 96, 128, 160$ for $l = 4$ and $L = 50, 60, 70, 80, 100, 120, 140$ for $l = 5$.

3. Results and discussion

3.1. Jamming coverage

Typical configurations corresponding to dimers (red and green circles) deposited on heterogeneous bivariate surfaces with chessboard (3_C) and random (2_R) topography are shown in Figs. 1 and 2, respectively. Black squares correspond to type 1 sites and white squares represent type 2 sites. The coverage degrees are $\theta_1 = 0.4$ and $\theta_2 = 0.6$ (Fig. 1) and $\theta_1 = 0.4$ and $\theta_2 = 0.7$ (Fig. 2).

As mentioned in the previous section, the irreversible deposition of objects occupying more than one lattice site leads to a final state (known as jamming state), in which no more objects can be deposited due to the absence of free space of appropriate size and shape. Then, for each value of θ_1 (θ_2), the coverage of the type 2 (1) sites can reach a maximum value (or jamming coverage), $\theta_2(=\theta_2^J < 1)[\theta_1(=\theta_1^J < 1)]$. Fig. 3 collects the limit values of θ_2 as a function of θ_1 for different topographies and lattice sizes as indicated. In this case, θ_1 is fixed at a given value and θ_2 is varied up to the jamming limit. Several conclusions can be drawn from the figure.

The coverage of the type 1 sites varies between 0 and θ_1^J ($0 \le \theta_1 \le \theta_1^J$). As it can be easily understood, θ_1^J corresponds to the value of the jamming coverage of dimers on a homogeneous square lattice $\theta_1^J \approx 0.907$ [42]. In the limit $\theta_1 \to 0$ (region not shown in Fig. 3 for clarity), the corresponding value of θ_2 represents the maximum concentration of occupied sites that is possible to reach on the type 2 patches. This value (1) depends on size and distribution of the patches, (2) increases for increasing values of l [45] and (3) as expected, tends to 0.907 for $l \to \infty$ (independent of the distribution of the patches).

On the other hand, in the limit $\theta_1 \to 0.907$, all curves converge to a point ($\theta_1^J = \theta_2^J = 0.907$). In fact, the condition $\theta_1 = \theta_2$ restricts the filling process to the first stage (when a coverage θ_1 is reached on the type 1 patches, then a coverage $x = \theta_1 = \theta_2$ is also reached on the type 2 patches) and the problem reduces to the homogeneous case. Thus, the extreme point ($\theta_1^J = \theta_2^J = 0.907$) is a particular case of the condition $\theta_1 = \theta_2$, and does not depend on the topography.

In the intermediate range of θ_1, most of curves exhibit a non-monotonic behavior: they decrease for small values of θ_1, goes through a minimum, and finally asymptotically converges towards the limit θ_1 point ($\theta_1^J = \theta_2^J = 0.907$). Strong size effects are observed for random topography and $l = 1$, where the corresponding curve grows linearly in all range of θ_1.

With respect to the influence of the topography, it is interesting to note that the behavior of a curve corresponding to a random topography of size l seems to approach that of a chessboard topography with an effective size $l_{eff} > l$. This characteristic has been previously reported in studies of adsorption on heterogeneous surfaces [38]. As $l \to \infty$, the border effects between the patches disappear and the curves converge to a limit curve (dashed line in Fig. 3), independently of the distribution of the patches.

Since the problem is invariant under the transformation $\theta_1 \to \theta_2$ and $\theta_2 \to \theta_1$, similar results to those reported in Fig. 3 can be obtained by fixing θ_2 and varying the coverage of the type 1 sites up to the jamming density. The corresponding

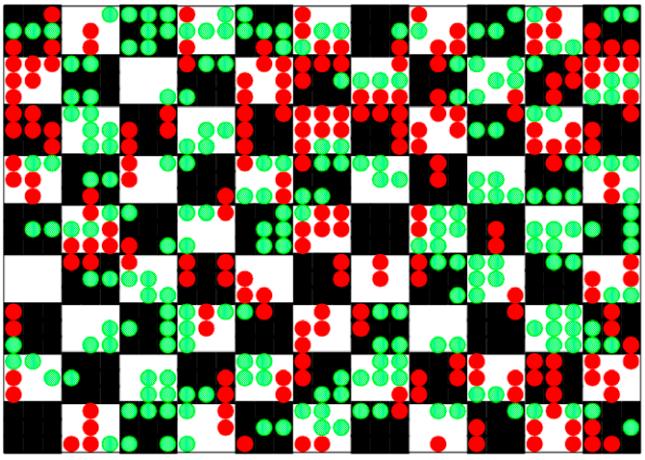

Fig. 1. Snapshot of a portion of a typical configuration of dimers deposited on a heterogeneous bivariate surfaces with chessboard topography (with $l = 3$), $\theta_1 = 0.4$ and $\theta_2 = 0.6$. Black squares and white squares correspond to type 1 sites and type 2 sites, respectively. Red circles and green circles correspond to vertical and horizontal dimers, respectively. (For interpretation of the references to color in this figure legend, the reader is referred to the web version of this article.)

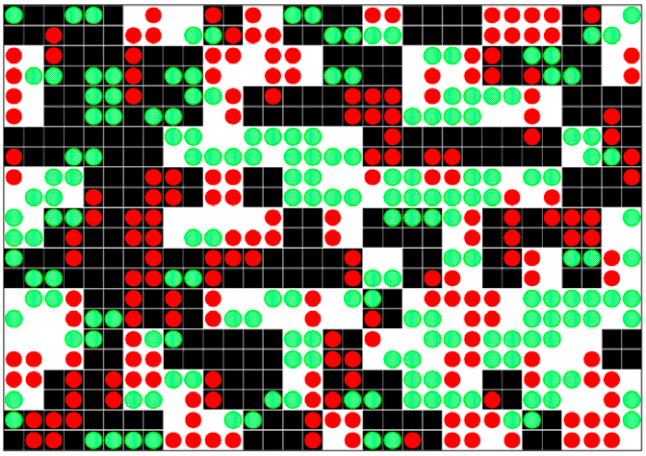

Fig. 2. Same as in Fig. 1 for a random topography (with $l = 2$), $\theta_1 = 0.4$ and $\theta_2 = 0.7$. (For interpretation of the references to color in this figure legend, the reader is referred to the web version of this article.)

curves delimit the region of available values of θ_1 and θ_2. This situation is shown in Fig. 4 for a 2_C topography. As it can be observed, the area of the allowed region diminishes with respect to the corresponding one for the case of percolation of monomers, where θ_1 and θ_2 vary in the range [0, 1] [34].

3.2. Percolation phase diagram

Once the θ_1–θ_2 parameter space is determined, the percolation properties of the system can be studied.

In Fig. 5(a), the percolation probability $R_L^U(\theta_2)$ is shown for a typical case: $\theta_1 = 0.5$, 4_C topography and different values of L as indicated. It can be seen that $R_L^U(\theta_2)$ increases as θ_2 increases for all sizes of the system. On the other hand, as L increases, the jump (between non-percolating and percolating state) becomes more pronounced and the curve displaces to higher values of θ_2.

The standard theory of finite-size scaling allows for various efficient routes to estimate the percolation threshold from MC data [2,28,43,44]. One of this method, which will be used here, is from the extrapolation of the positions $\theta_2^c(L)$ of the maxima of the slopes of $R_L^U(\theta_2)$. For each size, $dR_L^U(\theta_2)/d\theta_2$ is calculated and fitted by a Gaussian function. The corresponding value of $\theta_2^c(L)$ is obtained from the central point of the Gaussian function, see inset in Fig. 5(b). For this quantity one expects that

$$\theta_2^c(L) = \theta_2^c(\infty) + AL^{-\frac{1}{\nu}}, \quad \text{(fixed } \theta_1\text{)} \tag{1}$$

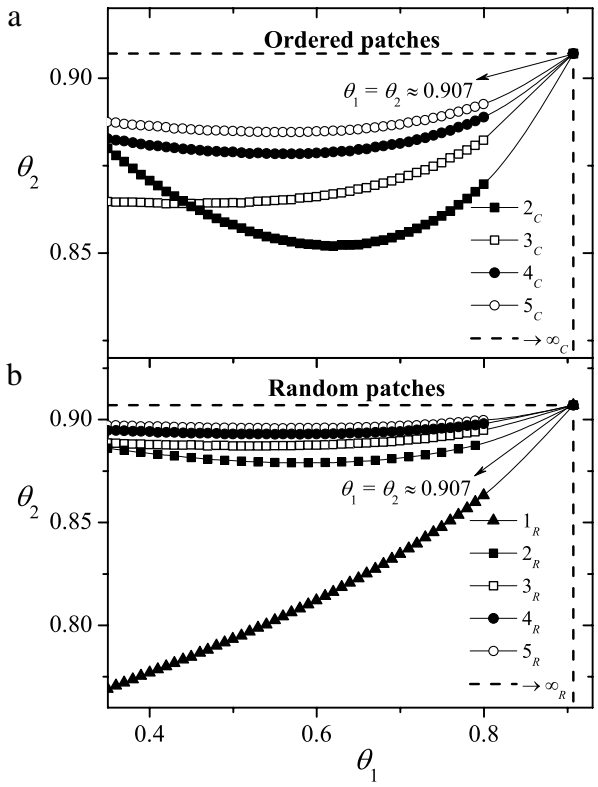

Fig. 3. Values of θ_2 at which jamming occurs as a function of θ_1 for chessboard [(a)] and random [(b)] topographies. The curves correspond to different values of l as indicated.

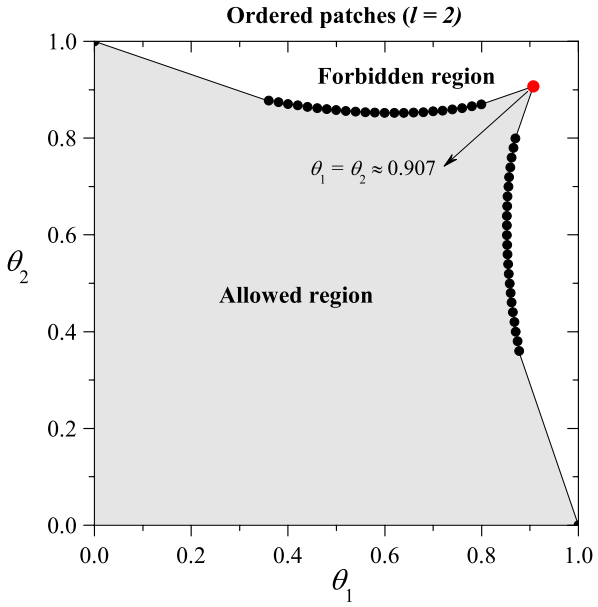

Fig. 4. Allowed and forbidden regions of the parameters θ_1 and θ_2 for a 2_C topography.

where A is a non-universal constant and the critical exponent ν is expected to be equal to $\nu = 4/3$, as in the case of standard random percolation [2,8,9]. The interested reader is invited to see Refs. [28,43,44] for a more detailed discussion of the method for determining the critical threshold and the critical exponents.

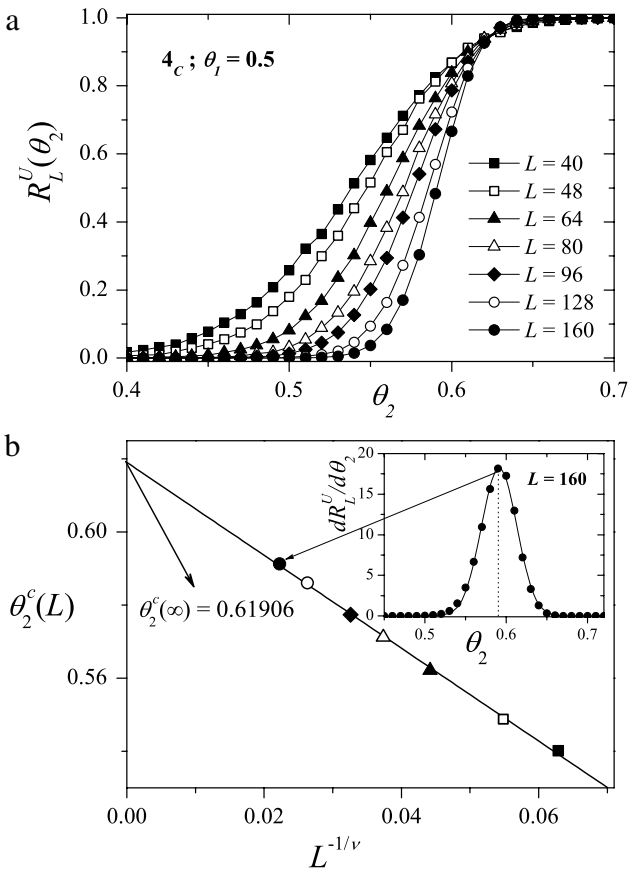

Fig. 5. (a) Fraction of percolating lattices $R_L^U(\theta_2)$ as a function of θ_2 for ordered patches with $l = 4$, $\theta_1 = 0.5$ and different values of L as indicated. (b) Extrapolation of $\theta_2^c(L)$ towards the thermodynamic limit according to the theoretical prediction given by Eq. (1). Inset: $dR_L^U(\theta_2)/d\theta_2$ and the corresponding Gaussian fitting curve for a 4_C topography, $\theta_1 = 0.5$ and $L = 160$.

Fig. 5(b) shows the extrapolation towards the thermodynamic limit of $\theta_2^c(L)$ according to Eq. (1) for the data in Fig. 5(a). In this case, $\theta_2^c(\infty) = 0.61906$. This is the way of obtaining the percolation threshold for each topography and each particular value of l and θ_1.

In Fig. 6(a), the finite-size scaling analysis has been used in the whole range of the variables (θ_1 and θ_2) in order to determine the percolation thresholds and the phase diagram in the case of ordered patches with $l = 2$. Thus, the resulting (θ_1–θ_2) phase diagram (solid circles) is shown in the figure, in comparison with the corresponding critical line for monomers (empty circles) on a 2_C surface.

As previously discussed, the problem is invariant under the transformation $\theta_1 \rightarrow \theta_2$ and $\theta_2 \rightarrow \theta_1$. Consequently, the critical lines separating the percolating and non-percolating regions are symmetrical under mirror reflection about the line $\theta_1 = \theta_2$. On this line, the system behaves as a homogeneous one. This property can be observed in the figure by noting that the line $\theta_1 = \theta_2$ cuts the critical lines corresponding to monomers and dimers in the points ($\theta_1 \approx \theta_2 \approx 0.593$) and ($\theta_1 \approx \theta_2 \approx 0.564$), respectively. The value 0.593 represents the percolation threshold of monomers on homogeneous square lattices [2], while the value 0.564 corresponds to dimers on homogeneous square lattices [8,9].

Fig. 6(a) shows also that the more important qualitative and quantitative differences between the results for monomers and dimers are related to jamming effects. The restrictions in the (θ_1–θ_2) space, due to the blocking of the lattice by the already randomly deposited dimers, lead to a decrease in the dimer percolating area with respect to the case of monomers.

The effect of the topography on the percolation phase diagram of dimers on bivariate heterogeneous surfaces is presented in Fig. 6(b). The study indicates that: (1) for all cases, the values of θ_2 on the critical line decrease for increasing values of θ_1; (2) the critical pair ($\theta_1 \approx 0.564$, $\theta_2 \approx 0.564$) belongs to all transition lines because the percolation threshold of dimers deposited on a homogeneous square lattice is 0.564 [8,9]; (3) for a fixed value of θ_1 and a given distribution (ordered or random) of patches, the critical value of θ_2 decreases as the patch size is increased; (4) for a fixed value of l and θ_1, the corresponding critical value of θ_2 for random patches is smaller than for ordered patches; and (5) for high values of l, the problem does not depend on lattice details and the critical lines tend to a limit curve for the limit $l \rightarrow \infty$.

The results in Fig. 6 prove that the geometrical distribution of sites is an important property to be taken into account in percolation problems, and here means that percolation is favored by a random distribution of patches.

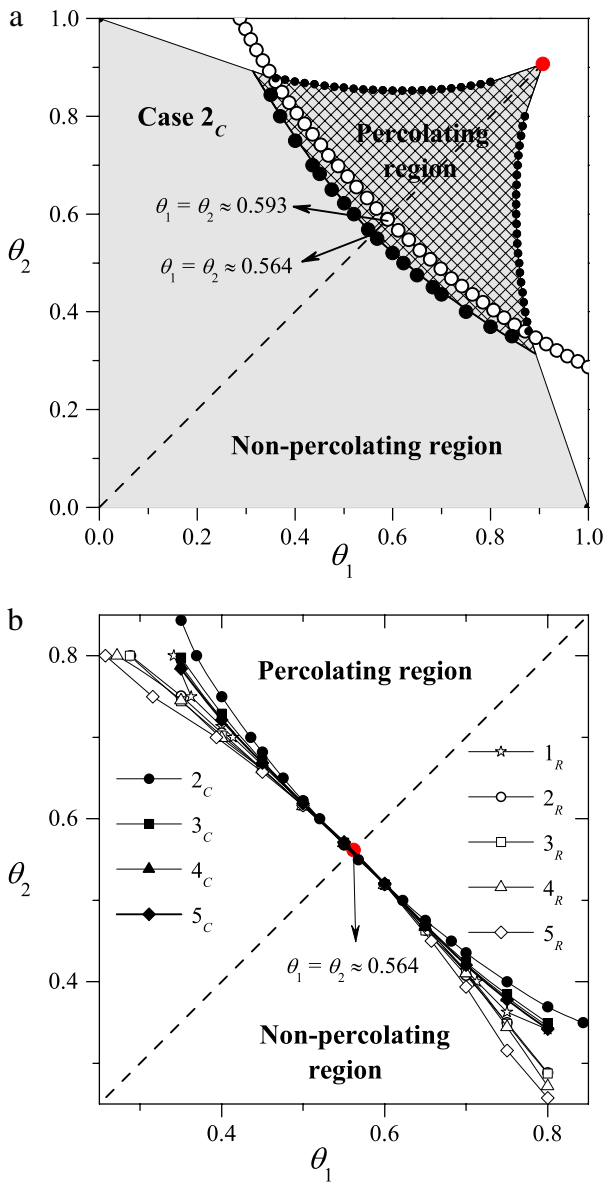

Fig. 6. (a) Percolation phase diagram of dimers on a 2_C surface. Solid circles joined by a connecting line separate the percolating and non-percolating regions. For comparison, the critical line corresponding to monomers on a chessboard surface with $l = 2$ is shown in open circles. (b) Critical lines separating the percolating and non-percolating regions for dimers deposited on surfaces with different topographies as indicated.

4. Conclusions

In this work, the percolation phase diagram of irreversibly deposited dimers on heterogeneous square lattices is addressed by using irreversible adsorption simulations and finite-size scaling analysis. The surfaces are represented by two kinds of sites: type 1 and type 2 sites form $l \times l$ patches, which can be either arranged in a deterministic chessboard structure or in a random way. Thus, the system is characterized by the distribution (ordered or random) of the patches, the patch size l and the probability of occupying each patch θ_i ($i = 1, 2$).

At high coverage, the final state generated by irreversible adsorption of dimers is a disordered state (known as jamming state), in which no more objects can be deposited due to the absence of free space of appropriate size and shape. As a consequence of this effect, the space of the parameters θ_1 and θ_2 is restricted for values of coverage close to 1. Then, as a first step to calculate the phase diagram, the curves limiting the region of available values of θ_1 and θ_2 were obtained for the different studied topographies. The results revealed a strong dependence of the limit curves on topography.

In a second step, the critical curves separating the percolating and non-percolating regions were calculated for different values of the parameters of the system. The results (1) absolutely agree in all limits with the corresponding ones from

classical dimer percolation; (2) show that the transition lines are largely affected by the size of the patches as well as by their geometrical distribution; and (3) indicate that percolation is favored by a random distribution of patches.

Acknowledgments

This work was supported in part by CONICET (Argentina) under project number PIP 112-201101-00615; Universidad Nacional de San Luis (Argentina) under project 322000; and the National Agency of Scientific and Technological Promotion (Argentina) under project PICT-2010-1466. The numerical work were done using the BACO parallel cluster (composed by 50 PCs each with an Intel i7-3370/2600 processor) located at Instituto de Física Aplicada, Universidad Nacional de San Luis - CONICET, San Luis, Argentina.

References

[1] J.M. Hammersley, Proc. Camb. Phil. Soc. 53 (1957) 642.
[2] D. Stauffer, A. Aharony, Introduction to Percolation Theory, Taylor & Francis, London, 1994.
[3] G. Deutscher, R. Zallen, J. Adler (Eds.), Percolation Structures and Processes, in: Annals of the Israel Physical Society, vol. 5, Hilger, Bristol, 1983.
[4] M. Sahimi, Applications of Percolation Theory, Taylor & Francis, London, 1992.
[5] R. Zallen, The Physics of Amorphous Solids, John Wiley & Sons, New York, 1983.
[6] J.W. Essam, Rep. Progr. Phys. 43 (1980) 843.
[7] J.P. Hovi, A. Aharony, Phys. Rev. B 53 (1996) 235.
[8] V. Cornette, A.J. Ramirez-Pastor, F. Nieto, Phys. A 327 (2003) 71.
[9] V. Cornette, A.J. Ramirez-Pastor, F. Nieto, Eur. J. Phys. B 36 (2003) 391.
[10] K. Binder, Rep. Progr. Phys. 60 (1997) 488.
[11] G. Grimmett, Percolation, Springer-Verlag, Berlin, 1999.
[12] B. Bollobás, O. Riordan, Percolation, Cambridge University Press, New York, 2006.
[13] Y. Gazit, D.A. Berk, M. Leunig, L.T. Baxter, R.K. Jain, Phys. Rev. Lett. 75 (1995) 2428;
J.W. Baish, Y. Gazit, D.A Berk, M. Nozue, L.T. Baxter, R.K. Jain, Microvasc. Res. 51 (1996) 327.
[14] D.S. Callaway, M.E.J. Newman, S.H. Strogatz, D.J. Watts, Phys. Rev. Lett. 85 (2000) 5468.
[15] S.N. Dorogovtsev, A.V. Goltsev, J.F.F. Mendes, Rev. Modern Phys. 80 (2008) 1275.
[16] A. Bashan, R. Parshani, S. Havlin, Phys. Rev. E 83 (2011) 051127.
[17] R.K. Pan, M. Kivelä, J. Saramäki, K. Kaski, J. Kertész, Phys. Rev. E 83 (2011) 046112.
[18] S. Kirkpatrick, Rev. Modern Phys. 45 (1973) 574.
[19] A. Yazdi, H. Hamzehpour, M. Sahimi, Phys. Rev. E 84 (2011) 046317.
[20] C. Moore, M.E.J. Newman, Phys. Rev. E 61 (2000) 5678.
[21] C.L. Henley, Phys. Rev. Lett. 71 (1993) 2741.
[22] M. Adam, M. Delsanti, D. Durand, G. Hild, J.P. Munch, Pure Appl. Chem. 53 (1981) 1489.
[23] E. Kenah, J.M. Robins, Phys. Rev. E 76 (2007) 036113.
[24] R. Cohen, K. Erez, D. ben Avraham, S. Havlin, Phys. Rev. Lett. 85 (2000) 4626.
[25] A.A. Moreira, J.S. Andrade, H.J. Herrmann, J.O. Indekeu, Phys. Rev. Lett. 102 (2009) 018701;
H. Hooyberghs, B. Van Schaeybroeck, A.A. Moreira, J.S. Andrade, H.J. Herrmann, J.O. Indekeu, Phys. Rev. E 81 (2010) 011102.
[26] Y. Chen, G. Paul, R. Cohen, S. Havlin, S.P. Borgatti, F. Liljeros, H.E. Stanley, Phys. Rev. E 75 (2007) 046107.
[27] S. Solomon, G. Weisbuch, L. de Arcangelis, N. Jan, D. Stauffer, Phys. A 277 (2000) 239.
[28] M.C. Gimenez, F. Nieto, A.J. Ramirez-Pastor, J. Phys. A: Math. Gen. 38 (2005) 3253.
[29] M.C. Gimenez, F. Nieto, A.J. Ramirez-Pastor, J. Chem. Phys. 125 (2006) 184707.
[30] M.C. Gimenez, A.J. Ramirez-Pastor, F. Nieto, Phys. A 387 (2008) 6526.
[31] M.C. Gimenez, A.J. Ramirez-Pastor, F. Nieto, Phys. A 389 (2010) 1521.
[32] G.D. Garcia, F.O. Sanchez-Varretti, P.M. Centres, A.J. Ramirez-Pastor, Eur. J. Phys. B 86 (2013) 403.
[33] Y.Y. Tarasevich, N.I. Lebovka, V.V. Laptev, Phys. Rev. E 86 (2012) 061116.
[34] F. Nieto, A.J. Ramirez Cuesta, R.J. Faccio, Phys. Rev. E 59 (1999) 3706.
[35] R.M. Ziff, E. Gulari, Y. Barshad, Phys. Rev. Lett. 56 (1986) 2553. and references therein.
[36] J.E. Davis, P.D. Nolan, S.G. Karseboom, C.B. Mullins, J. Chem. Phys. 107 (1997) 943.
[37] Z. Gao, Z.R. Yang, Physica A 255 (1998) 242.
[38] F. Bulnes, A.J. Ramirez-Pastor, G. Zgrablich, J. Chem. Phys. 115 (2001) 1513; Phys. Rev. E 65 (2002) 031603; Langmuir 23 (2007) 1264.
[39] T.W. Fishlock, J.B. Pethica, R.G. Eydell, Surf. Sci. 445 (2000) L47.
[40] F. Bulnes, F. Nieto, V. Pereyra, G. Zgrablich, C. Uebing, Langmuir 15 (1999) 5990.
[41] J. Hoshen, R. Kopelman, Phys. Rev. B 14 (1976) 3428.
[42] J.W. Evans, Rev. Modern Phys. 65 (1993) 1281.
[43] F. Yonezawa, S. Sakamoto, M. Hori, Phys. Rev. B 40 (1989) 636.
[44] F. Yonezawa, S. Sakamoto, M. Hori, Phys. Rev. B 40 (1989) 650.
[45] In the case of chessboard surfaces, point (2) is valid only for $l > 2$. The case 1_C does not make sense, and $\theta_2 = 1$ for 2_C surfaces with $\theta_1 = 0$.